Solution Dynamics in Aqueous Monohydric Alcohol Systems

William S. Price,*,† Hiroyuki Ide,‡ and Yoji Arata§,#

Department of Chemistry, Tokyo Metropolitan University, 1-1 Minami-Ohsawa, Hachioji, Tokyo 192-0397, Japan, FLW, Food Research & Development Laboratories, Ajinomoto Co., Inc. 1-1, Suzuki-cho, Kawasaki-ku, Kawasaki-shi 210-8681, Japan, and Water Research Institute, Sengen 2-1-6, Tsukuba, Ibaraki 305-004, Japan

Received: October 21, 2002; In Final Form: April 7, 2003

The associative behavior of aqueous methanol, ethanol, and *tert*-butyl alcohol solutions at mole fractions ranging from 0 to 1 at 273, 283, and 298 K was examined using PGSE NMR measurements of the self-diffusion coefficients of the alkyl group, water and, depending on the exchange rate, hydroxyl protons. The results show that *tert*-butyl alcohol has the greatest ability to stabilize water through hydrophobic hydration than methanol or ethanol due to the more ideal fit of the *tert*-butyl group to the structure of water. However, at higher concentrations *tert*-butyl alcohol is the least able to cohesively interact with water through hydrogen bonding. The results provide compelling evidence for alcohol self-association (methanol < ethanol < *tert*-butyl alcohol) in very dilute solution. The alcohol molecules can be likened to very short lipid molecules undergoing complicated solution interactions due to their amphiphilic nature.

Introduction

Many of the anomalous physical properties observed in liquids are related to inhomogeneities at the microscopic level.[1,2] Monohydric alcohol−water mixtures have long attracted attention due not only to their ubiquitous nature, but also to their importance as model systems: the amphiphilic nature of alcohol molecules makes them excellent probes for studying water structure, since through hydrogen bonding, they strongly interact with water and modulate the clathrate-like structures that form in pure water.[3−5] Also, depending on the size and arrangement of their alkyl groups, the alcohol molecules perturb the water structure through steric and hydrophobic interactions ("hydrophobic hydration").[6] Indeed, "premicellar" hydrophobic interactions are the dominant factor in the molecular dynamics of microheterogeneity.[7] Consequently, clarification of the noncovalent association in monohydric alcohols is useful for understanding the self-assembly of micelle systems and protein stabilization and denaturation.

Due to their close structural similarity, methanol (MeOH), ethanol (EtOH), and *tert*-butyl alcohol (TBA) is an obvious set of monohydric alcohols to contrast, with TBA being the most hydrophobic alcohol that is miscible with water at all alcohol mole fractions, x_A. Solutions of these alcohols have been studied using a variety of techniques including density,[8] dielectric relaxation,[6,9] dynamic light scattering,[10] compressibility,[11−15] IR,[8,12,13,16−18] molecular dynamic (MD) simulations,[19−24] mutual diffusion measurements,[25] tracer diffusion,[8] neutron diffraction,[22] integral equation theory,[26] MS and XRD,[17,27] thermodynamics measurements,[14,28] and viscosity.[29] Yet, the solution behavior of these monohydric alcohol systems remains controversial.

NMR-based techniques are information rich and noninvasive. Many of the NMR measurements of these alcohol systems have involved chemical shift measurements (e.g., refs 16, 18, 30, and 31), but the data interpretation is complicated by the need to correct for the x_A-dependent changes in bulk magnetic susceptibility.[18,31] Since the self-diffusion coefficient of a single molecule is directly related to molecular size and solute−solvent interactions, it provides particularly direct information on solution structure. Pulsed gradient spin−echo (PGSE) NMR[32,33] is a very convenient technique for measuring self-diffusion. From fluorescence measurements, it is known that the monohydric alcohol aggregates have lifetimes of less than 1 μs,[34] which is much shorter than the PGSE time scale (tens of milliseconds). Thus, the measured diffusion coefficient of a species reflects a time-average over all of its association states. Although some studies have used fully protonated samples, most have used deuterated species and sometimes in combination with ^{1}H NMR relaxation measurements to calculate the "association parameter" A_{22}.[35−39]

Here, PGSE measurements were used to comprehensively probe these three aqueous alcohol systems over the entire concentration range at 273, 283, and 298 K. Since undeuterated alcohols and water were used, the diffusion coefficients of the water, D_W, the hydroxyl proton, D_{OH}, or in the case of fast exchange between water and hydroxyl protons, the average diffusion coefficient of the water and hydroxyl protons, D_{WOH}, were measured in addition to the alcohol diffusion coefficient, D_A. In addition, the ^{1}H chemical shifts of the species relative to that of the methyl group, δ_{diff}, were obtained. The data provide detailed clarification as to where the alcohol and water stop behaving like pure liquids, how their hydration shells interact and how this is affected by the different size and geometry of the alcohol molecules.

* Corresponding Author: Dr. William S. Price, Department of Chemistry, Tokyo Metropolitan University, 1-1 Minami-Ohsawa, Hachioji, Tokyo 192-0397, Japan. Ph: +81 426 77 2555. FAX: +81 426 77 2525. E-mail: wprice@comp.metro-u.ac.jp.

† Tokyo Metropolitan University.

‡ Ajinomoto Co., Inc.

§ Water Research Institute.

Present address: Genomic Sciences Center, RIKEN, Ono 61-1, Tsurumi, Yokohama 230-0046, Japan.

10.1021/jp027257z CCC: $25.00
Published on Web 05/24/2003

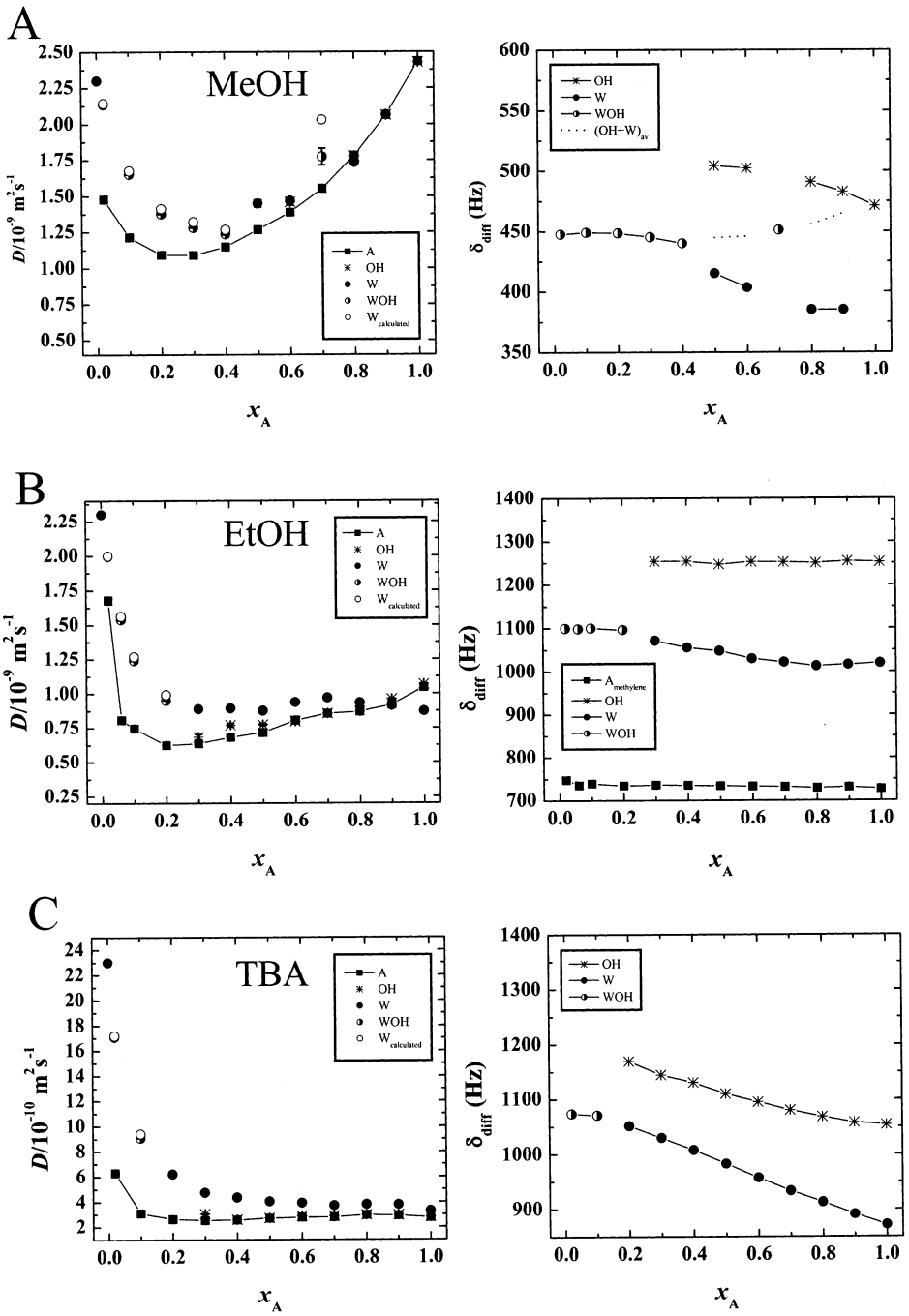

Figure 1. Diffusion coefficients (left) and chemical shift differences (right) of the alkyl group (■), hydroxyl (∗), water (experimental: ●; calculated: ○), and water-hydroxyl (◑) peaks with respect to the respective methyl resonance at 298 K at various x_A in the (A) methanol−water, (B) ethanol−water, and (C) *tert*-butyl alcohol−water systems. Error bars for the diffusion measurements are included; however, the errors are typically smaller than the symbols. The water diffusion coefficient at $x_A = 0$ for each of the three samples was interpolated from the data in ref 40. The dotted line represents extrapolation of the water-hydroxyl chemical shift calculated from the population-weighted average of the hydroxyl and water protons.

Experimental Section

Materials. Methanol (absolute grade) was from Sigma, ethanol (extra pure grade) was from Wako Pure Chemicals, and *tert*-butyl alcohol (extra pure grade) was from Nacalai Tesque. Reverse osmosis water was used to prepare the samples. For NMR measurements, samples were placed and flame sealed into 5-mm spherical microcells (529A; Wilmad, NJ). The compositions of the samples were verified from the ratio of the integrals of the resonances in a standard pulse-and-acquire NMR experiment.

NMR Measurements. ^{1}H PGSE NMR measurements were performed as described previously.[40] The Hahn spin−echo pulse sequence containing a "square" magnetic field gradient pulse of duration δ and magnitude g in each τ period was used for the translational diffusion measurements. The separation between the leading edges of the gradient pulses, Δ, which defines the time scale of the diffusion measurement was set to 30 ms. Typically, δ was set to 4 ms and 13 increments of g in the range of 0 to 0.5 Tm^{-1} were used with four scans being averaged for each value of g. For a single diffusing species, the echo signal attenuation, E, is related to the diffusion coefficient, D, by

$$E = \exp(-\gamma^2 g^2 D\delta^2(\Delta - \delta/3)) \quad (1)$$

TABLE 1: Characteristic Points in the Diffusive Behavior of the Three Alcohol Systems[a]

	methanol-H_2O			ethanol-H_2O			*tert*-butanol-H_2O			H_2O
T (K)	$D_{A\,x_A=1}$ ($\times 10^{-9}$ m^2 s^{-1})	x_A of $D_{A\,min}$	x_A of D_{Wmin}	$D_{A\,x_A=1}$ ($\times 10^{-10}$ m^2 s^{-1})	x_A of D_{Amin}	x_A of D_{Wmin}	$D_{A\,x_A=1}$ ($\times 10^{-10}$ m^2 s^{-1})	x_A of D_{Amin}	x_A of D_{Wmin}	$D_{W\,x_A=0}$ ($\times 10^{-9}$ m^2 s^{-1})
298.0	2.44	0.25 (45)	0.40 (55)	10.5	0.20 (59)	0.30 (39)	2.77	0.3 (92)		2.30
283.4	1.88	0.23 (38)	0.35 (53)	7.6	0.20 (46)	0.30 (35)	1.14	0.3 (102)		1.59
273.1	1.59	0.20 (31)	0.30 (52)	5.9	0.20 (36)	0.30 (30)		0.3 (NA)		1.10

[a] $D_{A\,x_A=1}$ is the diffusion coefficient of the pure alcohol. The number in brackets following the value of x_A where diffusive minima occur represents the ratio ($D_{A\,min}/D_{A\,x_A=1}$ or $D_{W\,min}/D_{W\,x_A=0}$) as a percentage.

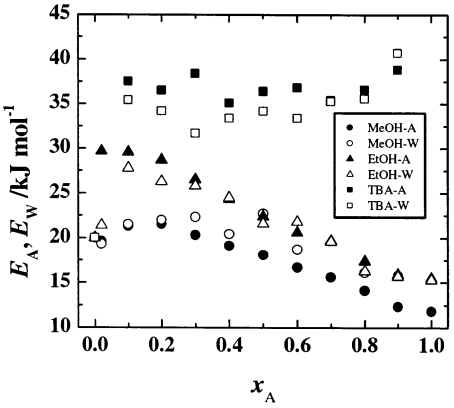

Figure 2. Approximate values for the Arrhenius activation energies for the translational motion of the alcohol (E_A; solid) and water (E_W; open) molecules for methanol (circle), ethanol (triangle), and TBA (square) systems calculated using the values of D_A and D_W (see Figure 1).

where γ is the gyromagnetic ratio. D was determined by regressing eq 1 onto the spin−echo attenuation data (i.e., resonance integrals). All of the PGSE data were well described by a single exponential. In the case of fast exchange where the water resonance coalesced with the hydroxyl resonance, the water diffusion coefficient was determined from

$$D_{Wcalc} = \frac{(2 - x_A)D_{WOH} - x_A D_A}{2(1 - x_A)} \qquad (2)$$

Chemical shifts were determined from simple pulse-and-acquire spectra with respect to the (intramolecular) alcohol methyl resonances to reduce the errors resulting from sample composition-dependent magnetic susceptibility differences.

Results and Discussion

Diffusion. The diffusion coefficients of the various species and the chemical shifts in the three alcohol systems were measured at 273.1, 283.4, and 298 K. Due to the higher freezing point of TBA, NMR measurements could not be performed on neat TBA at 273 K. Some species were not measurable in the PGSE experiment due to exchange-induced relaxation. As an example, the diffusion data from the 298 K measurements are graphed in Figure 1 and some of the characteristic points of the diffusion data for the three temperatures are summarized in Table 1. The present data agree well with previous measurements where the experimental conditions are sufficiently close to allow valid comparisons and/or allowance is made for the increased viscosity in deuterated systems (e.g., refs 8, 36, 37, 39, 41, and 42). Approximate values for the activation energies for the translational motion of the alcohol (E_A) and water (E_W) molecules were determined using the D_A and D_W values obtained at the three temperatures and are given in Figure 2. The activation energy for pure water, E_{H_2O}, (although in reality non-Arrhenius) ranges from 16.6 kJ mol^{-1} at 298 K to 21.5 kJ mol^{-1} at 273 K,[40] or 20 kJ mol^{-1} if calculated from the diffusion coefficients at the same temperatures used here.

Apart from the magnitudes of the diffusion coefficients, the three alcohol systems exhibited similar trends; consequently, the methanol system is considered in detail and only the points of distinction of the ethanol and TBA systems are subsequently discussed. Starting from $x_A = 0$, D_A rapidly decreases to a minimum ($D_{A\,min}$) at $x_A \sim 0.25$ and then gradually increases to the value for neat methanol ($D_{A\,x_A=1}$). At low x_A only D_{WOH} can be determined experimentally; however, D_{Wcalc} is only slightly greater than D_{WOH}. The behavior of D_W is similar to D_A, but there are some distinct differences. At low x_A, the condition $D_W > D_A$ holds, but D_W decreases to a minimum value ($D_{W\,min}$) at $x_A \sim 0.4$ (i.e., significantly later than D_A) and almost converges with D_A. At $x_A = 0.5$ and 0.6 the water and hydroxyl resonances are partially distinct but coalesce again at $x_A = 0.7$ and become distinct for $x_A > 0.7$. D_W at $x_A = 0.5$ and 0.6, and D_{OH} at $x_A = 0.6$ ($x_A = 0.5$ is unmeasurable) are slightly but significantly greater than D_A. At $x_A = 0.7$ D_{WOH} and D_{Wcalc} become much greater than D_A (NB D_A changed smoothly with x_A). However, by $x_A = 0.8$ $D_{OH} \sim D_A$ and, surprisingly, $D_W < D_A$, D_{OH}. At $x_A = 0.9$ $D_A \sim D_W$, but at lower temperatures the condition $D_W < D_A$ holds at both $x_A = 0.8$ and 0.9. Apart from decreases in magnitude, the overall behavior is largely temperature independent with only a small shift of the position of $D_{A\,min}$ and $D_{W\,min}$ to lower x_A. Starting from low x_A, E_A and $E_W = E_{H_2O}$ and then increase to reach maxima at $x_A \sim 0.2$ and then increasingly divergently decrease to values significantly below E_{H_2O} with $E_W > E_A$.

D_A and D_W converge at larger x_A in the EtOH and TBA systems in order of increasing size of the alkyl group. D_A and D_W exhibit clear minima in the ethanol system, but only D_A exhibits a minimum in the TBA system. In contrast to the two smaller alcohols, D_A in the TBA system reaches a local maximum at $x_A = 0.8$. This maximum has also been noted at 301 K.[36] In the ethanol system, it was possible to measure the diffusion of the trace quantity of water present in the neat sample (i.e., $x_A = 1$) and remarkably $D_W < D_A$. In the TBA system, the water resonance was distinct at all but the lowest x_A but distinct at 273 K at all x_A and, in contrast to the smaller alcohols, the condition $D_W > D_A$ always held. Although "macroscopically" miscible, the greater independence of D_A and D_W, especially at low x_A, in the TBA system implies that this system might be approaching immiscibility. While the hydroxyl proton is in fast exchange with the water protons at low x_A in the methanol and ethanol systems, the exchange is considerably slower in the TBA system and thus D_{OH} is measurable from lower x_A, where it is close to D_W, and as x_A increases from 0.2 to 0.4 it converges to D_A.

E_A and E_W increase much more rapidly with x_A in the ethanol and TBA systems. In the ethanol system, E_A and E_W reach maxima at $x_A \sim 0.1$ before decreasing to below E_{H_2O}, but different than the methanol system, E_A and E_W do not diverge.

Despite the larger error in the estimates of E_A and E_W for the TBA system, it is clear that after the rapid initial increase to almost twice E_{H_2O}, E_A and E_W remain roughly constant, in distinct contrast to the methanol and ethanol systems.

Stokes Radii. Although not strictly applicable due to the close relative sizes of the species, the Stokes−Einstein equation (stick boundary condition), viz.

$$D = \frac{kT}{6\pi\eta r} \tag{3}$$

where k is the Boltzmann constant and η (Pa s) is the solvent viscosity, provides a framework for discussing the alcohol diffusion data in terms of solution structure. Assuming that the effective hydrodynamic radius, r, is proportional to $\sqrt[3]{Mw}$, the equation predicts that in very dilute solution the difference in diffusion coefficient between the three alcohols should be less than a factor of 2 (NB the radii of MeOH, EtOH, and TBA derived from the molar volumes are 2.5, 2.8, and 3.4 Å, respectively); however, in reality the difference is much larger as shown in Figure 1 (e.g., at 298 K $D_{A\,min} = 1.1 \times 10^{-9}$ m^2 s^{-1} MeOH, 0.6×10^{-9} m^2 s^{-1} EtOH, and 2.6×10^{-10} m^2 s^{-1} TBA). Since D_W is also drastically decreased at low x_A, although to different extents in each system, the differences in diffusive behavior between the three alcohols must result from large differences in alcohol−water interactions together with some contribution from alcohol self-association. Alcohol self-association alone, however, cannot explain the large stabilizing effect on the water structure that is revealed by the dramatic decreases in D_W at low x_A. Whereas intermolecular interactions should affect the solution viscosity, increased alcohol self-association at low x_A should only affect D_A.

The normalized Stokes radii for the alcohol r_A and water r_W derived from eq 3 and literature values for the viscosities for the three systems are plotted in Figure 3. In each case, there is an initial very large increase in η which reaches a maximum at $x_A \sim 0.3$ before decreasing in the case of methanol and ethanol but with a very slight rise in the case of TBA at high x_A. In the case of methanol, r_A decreases with x_A and reaches a minimum at $x_A \sim 0.3$ before increasing to its pure solution (i.e., maximum) value. Whereas r_W initially decreases and then gradually rises to a value almost 50% larger than the value in pure water. r_W in the ethanol system behaves similarly to that in the methanol system except that the decrease at low x_A and the subsequent increase are much more pronounced; r_A has a local maximum at $x_A = 0.06$. The behavior of r_A and r_W in the TBA system closely follow the ethanol system, and at low x_A there is now an even more pronounced increase in r_A to a value significantly larger than its value in pure TBA. However, no local maximum was observed for r_A at low x_A, although this could be a consequence of insufficient sampling of the low x_A region.

Alcohol Solution Dynamics. *Methanol.* The decrease of both D_A and D_W at low x_A indicates there is significant interaction between the methanol and water molecules. D_A reaching a minimum before D_W implies the formation of hydration structures around the alcohol molecules. The proportion of the water that can be stabilized will depend on both x_A and the number of water molecules that can hydrate around an alcohol molecule. As x_A increases, a point is reached before all of the water molecules can be incorporated into such hydration structures where it is thermodynamically just as favorable for a water molecule to remain in solution or to enter a hydration shell. When there are insufficient water molecules to form hydration shells, alcohol self-association ("micellization") might become favorable. Indeed, integral equation theory and MD simulations[26] indicate a slight preference for water molecules to pack around the methanol oxygen group compared to the methanol methyl group. Consequently, the hydration structures become less well-defined, although the water as a whole is still more structured than pure water and D_A starts to increase slightly before D_W has reached a minimum. The low r_A values at low x_A indicate that methanol does not undergo significant self-association, which is as expected since, of the three alcohols, methanol is capable of forming the strongest hydrogen bonds with water due to its smaller size and less steric hindrance to the OH group and thus prefers to form 1:1 compounds with water.[9]

MD simulations imply that methanol is strongly solvated by a cage of water molecules at low x_A and occupies the interstitial

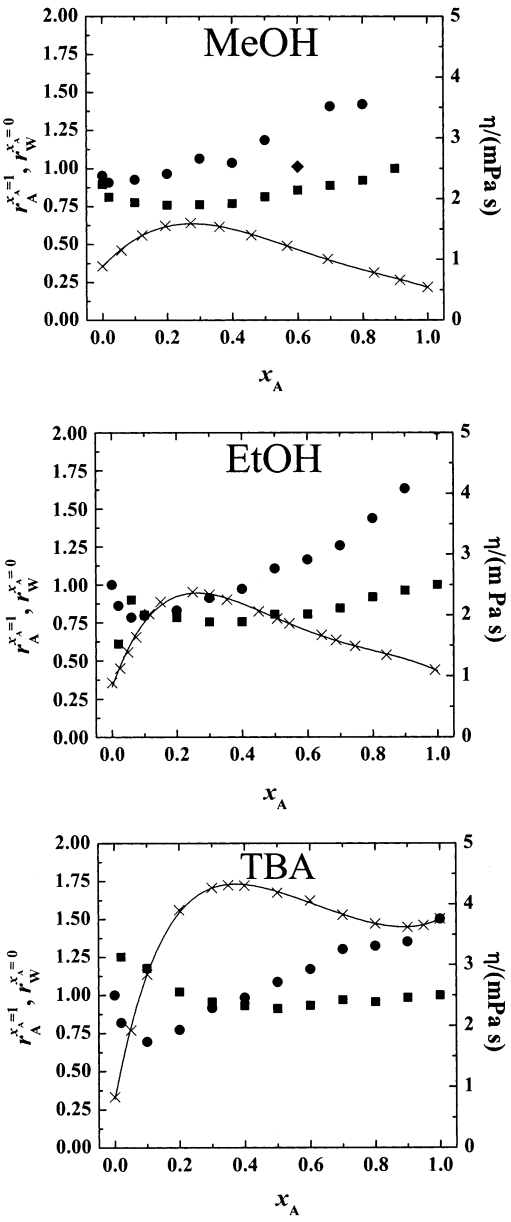

Figure 3. The effective radii of the alcohol (r_A, ■) and water (r_W, ●) determined from D_A, D_W, D_{Wcalc} and literature values of the solution viscosities (MeOH (298 K):[49] EtOH (298 K):[29] BuOH (301 K):[36]) using eq 3 for the methanol, ethanol, and butanol systems. Values of the solution viscosity at the same x_A used in the present work were determined by interpolation of the viscosity data (×) with a fifth order polynomial (–). The effective radii are normalized according to the respective pure solvent values. The value of r_W stemming from the $x_A = 0.7$ MeOH sample is less definite and is indicated by a solid diamond.

cavities in the water network, thereby retarding the diffusion of the water molecules.[21,23] The simulations also indicate that while methanol affects the water hydrogen-bond network, its influence does not extend past the first hydration shell.[23] On the basis of partial molar enthalpy data,[14] it was concluded that at low x_A the solute enhances the hydrogen bond network in its immediate vicinity, but diminishes the hydrogen bond probability in the bulk away from the solute, although the hydrogen bond network is connected throughout the bulk at any instance. These findings are consistent with the observation of $D_W > D_A$ at low x_A.

$x_A = 0.7$ corresponds to equal numbers of water and hydroxyl protons and thus the apparently anomalous increase in D_{OH} at $x_A = 0.7$ may correspond to the eversion from "methanol in water" to "water in methanol". The large D_{OH} value may simply be experimental error, but in support of the present data we note that the sample composition was verified from integrals of 1D NMR spectra and that D_A changed smoothly with x_A. Further, extrapolation of the calculated water-hydroxyl chemical shift calculated from the hydroxyl and water proton shifts (dotted line in Figure 1A) correctly predicts the chemical shift measured at $x_A = 0.7$.

At $x_A \geq 0.8$, the water molecules move independently of the alkyl group since although D_A and D_{OH} are very similar, D_W is significantly lower. This is in agreement with MD simulations,[21] indicating that at high x_A methanol retains most of its pure liquid structure. At high x_A, E_W tends to around 15 kJ mol^{-1} (see Figure 2), which is significantly less than E_{H_2O} but approaching the activation energy of isolated water molecules in nitromethane (10 kJ mol^{-1});[43] thus, at high x_A water is present either as isolated water molecules or as very small clusters.

Ethanol. The even larger decrease in D_A and D_W at low x_A than in the methanol system indicates even stronger alcohol−water interactions and again the lag in the decrease of D_W indicates the formation of clathrate-like hydrates. However, the spike in r_A at $x_A = 0.06$, which is at a considerably lower mole fraction than where $D_{A\,min}$ occurs ($x_A \sim 0.2$), is direct evidence for ethanol self-association. Maximum solution structuring occurs at the value of x_A corresponding to $D_{W\,min}$ and consequently $D_{A\,min}$ occurs at higher x_A than if the reduction in D_A was due solely to self-association. The strengthening of hydrogen bonds between water molecules surrounding the alkyl group and overall stabilization of the water structure with increasing x_A has also been indicated by chemical shift and molar excess entropy measurements.[16,18,28] Compressibility measurements at 298 K indicate that the ethanol is essentially monomeric for $x_A < 0.06$, and increasingly self-associated in the range $0.06 < x_A < 0.29$.[11−13] However, A_{22} parameter analysis indicates increased self-association with decreasing x_A, especially at higher temperatures.[37] This is consistent with the results of IR, MS, and XRD measurements,[17,27] which indicate significant self-association at $x_A \leq 0.03$ with dimerization being evident in very dilute solution ($x_A \approx 0.001$) consistent with a model of a hydrophobic core structure composed of coherent ethyl groups with a strong hydrogen-bonded cage of water. The activation enthalpy and entropy derived from dielectric measurements give a distinct maximum at $x_A = 0.22$,[6] which is, within experimental error, the same value of x_A where $D_{A\,min}$ occurs. Although mass spectra showed drastic changes for $x_A \leq 0.2$, the spectra changed only slowly with x_A above this.[17,27]

Compressibility measurements at 298 K indicate that above $x_A = 0.29$ the hydrophobic hydration effects become negligible and the H_2O loses its hydrogen bond network and mixes into the ethanol solution as a single molecule.[11−13] This transition from water molecules being predominantly involved with other water molecules to becoming isolated water molecules diffusing in the "dynamic alcohol matrix" explains the crossover of D_W and D_A at $x_A \sim 0.9$ and is consistent with the low value of E_W at high x_A. Water and ethanol form an azeotrope at $x_A = 0.89$ (95.57% ethanol by wt),[44] and thus it is interesting to speculate how the crossover in diffusion coefficients is related to azeotrope formation. The independence of D_W at high x_A supports the inability to find any evidence for the formation of water adducts to ethanol chains at high x_A,[8] but at variance with a report of the formation of strong hydrogen bonds between the water proton and hydroxyl oxygens at high x_A based on chemical shift measurements.[16,18] Thermodynamic measurements of the molar excess entropy also indicate an increase in the total number of hydrogen bonds at high x_A.[28] However, given that $D_A = D_{OH} > D_W$ at high x_A it is reasonable to surmise that the hydrogen bonds are only between the same species (i.e., presumably ethanol−ethanol).

tert-Butanol. D_A and D_W decrease most drastically at low x_A in the TBA system and again the decrease in D_W lags behind D_A. The very large r_A value at low x_A indicates significant TBA self-association. The drop in r_W at low x_A is much larger than that for methanol and slightly larger than that observed for ethanol. MD simulations[24] reveal that the *tert*-butyl group sterically limits water's ability to hydrogen bond to the hydroxyl group and consequently TBA's hydration structure. Nevertheless, the closer fit of the TBA alkyl group than of alkyl groups of methanol or ethanol to the interstitial cavities in the water structure provides a more potent source of stabilization as verified by MD simulations.[19,20] Chemical shift,[18,31] light scattering,[10] thermodynamic,[14] and IR and compressibility data[12−15] have also indicated structural enhancement associated with an increase in hydrogen-bonding in the immediate vicinity of the TBA, and that the enhancement tends toward some energetically favorable ordered structure in the neighborhood of $x_A = 0.1$. This is in close agreement with our data. It is noted that the ratio $D_{A\,min}/D_{A\,x_A=1}$ decreases with increasing temperature for the TBA system, which appears to be consistent with the earlier light scattering study where it was suggested that the clathrate-hydrate structure breaks down with increasing temperature.[10] Interestingly, this ratio increases with temperature for the two smaller alcohols (Table 1).

Previous studies, although conflicting in details, indicate that maximum TBA self-association occurs at very low x_A. A_{22} analysis indicates that maximum self-association occurs at $x_A = 0.02-0.03$,[39] whereas IR indicates that the aggregation threshold for TBA is $x_A = 0.025$,[45] while compressibility studies indicate increasing TBA self-association in the range $0.025 < x_A < 0.13$.[12,13] In contrast, MD simulations indicate that at $x_A = 0.02$ there was little tendency to aggregate but at $x_A = 0.08$ aggregates consisting of three or four molecules are formed.[24] There is also controversy as to the size of the aggregates with X-ray diffraction and light scattering studies indicating the formation of very large clusters (e.g., X-ray: $TBA(H_2O)_{28}$ at $x_A = 0.039$; light scattering: $TBA(H_2O)_{21}$ for $0 \leq x_A \leq 0.05$ and $(TBA)_5(H_2O)_{105}$ for $0.05 \leq x_A \leq 0.06$).[10,46] Large clusters (e.g, $TBA(H_2O)_{30}$ at $x_A = 0.032$) have also been postulated on the basis of diffusion data.[47] Smaller clusters such as penta- or hexahydrates of TBA have been inferred from dielectric and DSC measurements,[9] and similarly, neutron diffraction studies indicate that as x_A increases from 0.06 to 0.16 small clusters of 2−3 TBA increasing to 5−6 molecules.[48] From the magnitude of r_A, our data indicate the presence of only reasonable small

clusters. Nevertheless, analysis would be complicated by polydispersity of cluster size.

Neutron diffraction data indicate that the dominant contact between the TBA molecules is via headgroups as expected for a process driven by hydrophobic interactions.[48] Previous diffusion based studies[47] at very low x_A have indicated that r_A was independent of x_A at very low x_A and then decreased suddenly at $x_A = 0.033$. Consequently, the value $x_A = 0.032$, which was termed the critical clathrate concentration, would correspond to the point where all of the water molecules were incorporated into the hydration shell. As x_A increases past this point, there is insufficient water to form such hydration shells and consequently r_A decreases. In agreement with this, we note that r_W begins increasing soon after r_A starts to decrease at low x_A. It has been reasoned that if the decrease in r_A was smooth the decrease may result from the formation of short-lived micelle like species.[47] In the present work, r_A does decrease smoothly; however, earlier diffusion measurements at very low x_A[47] give an abrupt decrease inconsistent with the formation of transient micellar species. Solute−solute enthalpic interactions, H^E_{AA}, which measure the degree of attraction between the alcohol molecules, peak around $x_A = 0.04-0.06$ and increase dramatically in going from methanol (33 kJ mol^{-1}) to ethanol (73 kJ mol^{-1}) to TBA (350 kJ mol^{-1})[14] and is consistent with our diffusion data, as little or no self-association was noted for methanol, some self-association for ethanol, and very significant self-association for TBA.

Chemical shift studies have revealed that there is significant disruption to hydrogen bonding in the range $x_A = 0.63-0.71$ in the TBA system,[31] and, as for ethanol, this region marks the transition to isolated water molecules. Thus, the maximum in D_A observed around $x_A \sim 0.8$ may be a consequence of this concentration providing the weakest intermolecular interactions as it also marks a local viscosity minimum (see Figure 3C). Similar to ethanol and methanol, the divergence of r_A and r_W at high x_A likely indicate the existence of a "water in oil" type phase separation.

Conclusions

The results show unequivocally that the alcohols enter into clathrate-like hydrates at low x_A. This hydration process is complicated by alcohol self-association, which is most evident in the TBA system and results from the increased hydrophobic interactions stemming from its large alkyl group. As x_A increases, the hydrate structures become less well defined, and at very high x_A the solution dynamics of the water and alcohol molecules become increasingly independent.

References and Notes

(1) Stanley, H. E.; Buldyrev, S. V.; Canpolat, M.; Mishima, O.; Sadr-Lahijany, M. R.; Scala, A.; Starr, F. W. *Phys. Chem. Chem. Phys.* **2000**, *2*, 1551−1558.

(2) Xia, X.; Wolynes, P. G. *Phys. Rev. Lett.* **2001**, *86*, 5526−5529.

(3) Stillinger, F. H. *Science* **1980**, *209*, 451−457.

(4) Speedy, R. J.; Ballance, J. A.; Cornish, B. D. *J. Phys. Chem.* **1983**, *87*, 325−328.

(5) Walrafen, G. E.; Chu, Y. C. *J. Phys. Chem.* **1995**, *99*, 10635−10643.

(6) Petong, P.; Pottel, R.; Kaatze, U. *J. Phys. Chem. A* **2000**, *104*, 7420−7428.

(7) Rupprecht, A.; Kaatze, U. *J. Phys. Chem. A* **1999**, *103*, 6485−6491.

(8) Harris, K. R.; Newitt, P. J.; Derlacki, Z. J. *J. Chem. Soc., Faraday Trans.* **1998**, *94*, 1963−1970.

(9) Murthy, S. S. N. *J. Phys. Chem.* **1999**, *103*, 7927−7937.

(10) Iwasaki, K.; Fujiyama, T. *J. Phys. Chem.* **1977**, *81*, 1908−1912.

(11) Onori, G. *J. Chem. Phys.* **1988**, *89*, 4325−4332.

(12) D'Angelo, M.; Onori, G.; Santucci, A. *J. Chem. Phys.* **1994**, *100*, 3107−3113.

(13) Onori, G.; Santucci, A. *J. Mol. Liq.* **1996**, *69*, 161−181.

(14) Tanaka, S. H.; Yoshihara, H. I.; Ho, A. W. C.; Lau, F. W.; Westh, P.; Koga, Y. *Can. J. Chem.* **1996**, *74*, 713−721.

(15) Tamura, K.; Osaki, A.; Koga, Y. *Phys. Chem. Chem. Phys.* **1999**, *1*, 121−126.

(16) Mizuno, K.; Miyashita, Y.; Shindo, Y.; Ogawa, H. *J. Phys. Chem.* **1995**, *99*, 3225−3228.

(17) Nishi, N.; Takahashi, S.; Matsumoto, M.; Tanaka, A.; Muraya, K.; Takamuku, T.; Yamaguchi, T. *J. Phys. Chem.* **1995**, *99*, 462−468.

(18) Mizuno, K.; Kimura, Y.; Morichika, H.; Nishimura, Y.; Shimada, S.; Maeda, S.; Imafuji, S.; Ochi, T. *J. Mol. Liq.* **2000**, *85*, 139−152.

(19) Tanaka, H.; Nakanishi, K.; Touhara, H. *J. Chem. Phys.* **1984**, *81*, 4065−4073.

(20) Okazaki, S.; Touhara, H.; Nakanishi, K. *J. Chem. Phys.* **1984**, *81*, 890−894.

(21) Laaksonen, A.; Kusalik, P. G.; Svishchev, I. M. *J. Phys. Chem. A* **1997**, *101*, 5910−5918.

(22) Benmore, C. J.; Loh, Y. L. *J. Chem. Phys.* **2000**, *112*, 5877−5883.

(23) Dlugoborski, T.; Hawlicka, E.; Swiatla-Wojcik, D. *J. Mol. Liq.* **2000**, *85*, 97−104.

(24) Kusalik, P. G.; Lyubartsev, A. P.; Bergman, D. L.; Laaksonen, A. *J. Phys. Chem. B* **2000**, *104*, 9533−9539.

(25) Harris, K. R.; Goscinska, T.; Lam, H. N. *J. Chem. Soc. , Faraday Trans.* **1993**, *89*, 1969−1974.

(26) Kvamme, B. *Phys. Chem. Chem. Phys.* **2002**, *4*, 942−948.

(27) Nishi N.; Matsumoto, M.; Takahashi, S.; Takamuku, T.; Yamagami, M.; Yamaguchi, T. *Structures and Dynamics of Clusters*; Universal Academy Press: Tokyo, 1996; pp 113−120.

(28) Larkin, J. A. *J. Chem. Thermodynamics* **1975**, *7*, 137−148.

(29) Harris, K. R.; Lam, H. N. *J. Chem. Soc., Faraday Trans.* **1995**, *91*, 4071−4077.

(30) Kuppers, J. R.; Carriker, N. E. *J. Magn. Reson.* **1971**, *5*, 73−77.

(31) Kuppers, J. R. *J. Magn. Reson.* **1971**, *4*, 220−225.

(32) Stilbs, P. *Prog. NMR Spectrosc.* **1987**, *19*, 1−45.

(33) Price W. S. *Annual Reports on NMR Spectroscopy*; Academic Press: London, 1996; pp 51−142.

(34) Zana, R.; Eljebari, M. J. *J. Phys. Chem.* **1993**, *97*, 11134−11136.

(35) Kida, J.; Uedaira, H. *J. Magn. Reson.* **1977**, *27*, 253−259.

(36) Kipkemboi, P. K.; Easteal, A. J. *Bull. Chem. Soc. Jpn.* **1994**, *67*, 2956−2961.

(37) Sacco, A.; Holz, M. *J. Chem. Soc., Faraday Trans.* **1997**, *93*, 1101−1104.

(38) Harris, K. R.; Newitt, P. J. *J. Phys. Chem.* **1998**, *B 102*, 8874−8879.

(39) Mayele, M.; Holz, M.; Sacco, A. *Phys. Chem. Chem. Phys.* **1999**, *1*, 4615−4618.

(40) Price, W. S.; Ide, H.; Arata, Y. *J. Phys. Chem.* **1999**, *A 103*, 448−450.

(41) Derlacki, Z. J.; Easteal, A. J.; Edge, A. V. J.; Woolf, L. A.; Roksandic, Z. *J. Phys. Chem.* **1985**, *89*, 5318−5322.

(42) Hawlicka, E. *Ber. Bunsen-Ges. Phys. Chem.* **1983**, *87*, 425−428.

(43) Price, W. S.; Ide, H.; Arata, Y. *J. Chem. Phys.* **2000**, *113*, 3686−3689.

(44) *The Merck Index*, 13 ed.; Merck & Co., Inc.: New Jersey, 2001.

(45) Freda, M.; Onori, G.; Santucci, A. *J. Phys. Chem. B* **2001**, *105*, 12714−12718.

(46) Nishikawa, K.; Iijima, T. *J. Phys. Chem.* **1990**, *94*, 6227−6231.

(47) Hawlicka, E.; Grabowski, R. *Chem. Phys. Lett.* **1995**, *236*, 64−70.

(48) Finney, J. L.; Bowron, D. T.; Soper, A. K. *J. Phys.: Condensed Matter* **2000**, *12*, A123-A128.

(49) Feakins, D.; Bates, F. M.; Waghorne, W. E.; Lawrence, K. G. *J. Chem. Soc., Faraday Trans.* **1993**, *89*, 3381−3388.